Combined membrane aeration and filtration for energy- and space-efficient COD removal in water reuse

Timmer, Marijn J.; Vaz, Maria Inês; De Paepe, Jolien; De Corte, Iris Jiaqi; Perdigão, Marina E.; Straathof, Adrie J.J.; Van Winckel, Tim; Vlaeminck, Siegfried E.

DOI
10.1016/j.wroa.2025.100344

Publication date
2025

Document Version
Final published version

Published in
Water Research X

Water Research X 27 (2025) 100344

Contents lists available at ScienceDirect

Water Research X

journal homepage: www.sciencedirect.com/journal/water-research-x

Combined membrane aeration and filtration for energy- and space-efficient COD removal in water reuse

Marijn J. Timmer [a,b], Maria Inês Vaz [a,b], Jolien De Paepe [a,b], Iris Jiaqi De Corte [a,b], Marina E. Perdigão [c], Adrie J.J. Straathof [c], Tim Van Winckel [a,b], Siegfried E. Vlaeminck [a,b,*]

[a] Biobased Sustainability Engineering (SUSTAIN), Department of Bioscience Engineering, University of Antwerp, Groenenborgerlaan 171, 2020 Antwerpen, Belgium
[b] Centre for Advanced Process Technology for Urban Resource recovery (CAPTURE), Frieda Saeysstraat 1, 9052 Gent, Belgium
[c] Department of Biotechnology, Delft University of Technology, Van der Maasweg 9, 2629 HZ Delft, the Netherlands

ARTICLE INFO

Keywords:
Decentralization
Biofilm management
Source separation
Intensification
Greywater
Permeability

ABSTRACT

Due to climate change and increasing droughts, wastewater treatment and water reuse are gaining importance. Yet, the state-of-the-art bubble-aerated membrane bioreactor (BA-MBR) faces competitiveness challenges due to its high energy use and maintenance requirements, especially at small scale. This study investigates a novel membrane-aerated MBR (MA-MBR) that integrates membrane aeration and filtration to reduce energy consumption and system footprint, enabling resource-efficient non-potable reuse. The MA-MBR treated greywater for domestic reuse and achieved stable chemical oxygen demand (COD) removal efficiencies up to 95 % at high loading rates (up to 4 g L^{-1} d^{-1}) and produced effluent with biological oxygen demand (BOD_5) values below 5 mg L^{-1}, meeting stringent reuse standards. Biomass dynamics revealed two distinct forms: biofilm on aeration membranes and flocs in suspension. Coarse bubble scouring facilitated biofilm detachment, enabling solid retention time (SRT) control. Oxidation-reduction potential (ORP) was linked to the biomass detachment efficiency, with negative ORP reducing mixed liquor suspended solids (MLSS) after scouring 5–10 times compared to operation at positive ORP. Reattachment of flocs reduced MLSS levels by 90 % within 60 min. A 25 % lower transmembrane pressure (TMP) in the MA-MBR compared to the BA-MBR after 72 h indicated lower fouling rates. Microbial communities were distinctly different between biofilm and flocs, especially under negative ORP conditions. These findings suggest the MA-MBR as low-footprint, low-fouling alternative for carbon removal from wastewaters with relatively high COD/N-ratios, and may improve resource efficiency for non-potable water reuse, for instance in decentralized source-separation applications.

1. Introduction

With global water scarcity intensifying, innovative strategies for sustainable water management are essential (Sedlak, 2014; Damania et al., 2017). Wastewater reuse has emerged as a key approach to mitigate water stress, covering applications from municipal to industrial reuse (Metcalf and Eddy et al., 2007). Treated wastewater can be upgraded for potable or non-potable uses. While potable reuse faces hurdles, non-potable reuse addresses 50–80 % of domestic water demand, reducing strain on potable supplies (Friedler and Butler, 1996; Noutsopoulos et al., 2018) and benefiting from evolving legislation (California Code of Regulations, 2015; European Commission, 2022). Reuse standards focus on Biochemical oxygen demand in 5 days (BOD_5), Total suspended solids (TSS), turbidity, and pathogens, varying by application and region (European Commission, 2022). Limits for nitrogen (15–45 mg TN L^{-1}) and Chemical Oxygen Demand, (50–100 mg COD L^{-1}) apply for domestic reuse, while irrigation reuse may omit nitrogen limits due to fertilization benefits (Mainardis et al., 2022).

Treatment technologies for reuse combine biological processes with ultrafiltration. Conventional activated sludge (CAS) systems separate sludge before ultrafiltration (Verstraete and Vlaeminck, 2011). Bubble-aerated membrane bioreactors (BA-MBRs) integrate ultrafiltration, reducing space needs by ~50 % (Pearce, 2008). However, BA-MBRs operate at high mixed liquor suspended solids (MLSS) of 8–12 g volatile suspended solids (VSS) L^{-1} (Judd, 2010), and face high energy demands for aeration and membrane scouring, comprising up to 50 % of OPEX (Brepols et al., 2010; Gil et al., 2010). Filtration membrane fouling impacts performance, requiring advanced cleaning techniques, such as

* Corresponding author.
E-mail address: siegfried.vlaeminck@uantwerpen.be (S.E. Vlaeminck).

https://doi.org/10.1016/j.wroa.2025.100344
Received 28 December 2024; Received in revised form 25 February 2025; Accepted 14 April 2025
Available online 14 April 2025

backwashing, relaxation and chemical cleaning, which further increase OPEX (Lee et al., 2013; Jiang et al., 2019).

Biofilm reactors, such as moving bed biofilm reactors (MBBR) and membrane-aerated biofilm reactors (MABR), offer significant advantages by decoupling MLSS from high solid retention time (SRT). Moreover, MABRs enhance aeration efficiency by up to 75 % compared to bubble aeration, performing well at small scale due to scale-independent oxygen transfer efficiency (Syron and Casey, 2008; Syron and Heffernan, 2017).

However, in combinations of biofilm systems and MBR such as MBBR-MBR, mixed results were obtained, attributed to fouling issues from unregulated biofilm detachment and excessive shear on the carriers (Yang et al., 2009; Chen, Bi and Ng, 2016). In contrast, MABR-MBR (MA-MBR) systems may reduce fouling and maintenance costs as it can be operated with lower and more controllable shear forces. Careful SRT management can balance biofilm and suspended biomass, for instance by intermittent scouring the aeration membranes and subsequent wasting (Stricker et al., 2011; Bunse et al., 2023).

One place where MA-MBR implementation may be especially promising is decentralized greywater treatment for reuse. Decentralization minimizes water transport, reduces energy consumption, and benefits from greywater's lower nutrient and solid content (Larsen, Udert and Lienert, 2013; Boano et al., 2020). While BA-MBRs are effective for greywater treatment (Atanasova et al., 2017), they face higher energy demands and maintenance costs, because of the smaller scale and limited tank depth (Brepols, Schäfer and Engelhardt, 2010; Verrecht et al., 2010). The MA-MBR system may overcome these challenges with energy-efficient membrane aeration and reduced fouling. Its scale-independent oxygen transfer efficiency (OTE) lowers energy use at small scale, while the low solid load in greywater could reduce clogging and extend membrane lifespan.

This study explores MA-MBR integration, hypothesizing improved energy efficiency, footprint reduction, and fouling mitigation compared to BA-MBRs. An MA-MBR system was constructed and operated with limited membrane scouring to minimize MLSS exposure. COD loading optimization and effluent quality compliance were assessed. Transmembrane pressure was monitored for fouling, and microbial dynamics were analyzed to examine effects of organics loading rate (OLR), Oxidation-Reduction Potential (ORP), and SRT. Results were benchmarked against a BA-MBR system to validate performance enhancements in greywater treatment.

2. Results

An MA-MBR was operated for 200 d on complex synthetic greywater at OLR ranging from 0.5 to 6 g COD L^{-1} d^{-1} (Fig. 1) and the COD removal rates (CODRR), efficiencies (CODRE) and effluent quality were assessed and benchmarked to a BA-MBR system utilizing conventional bubble aeration.

2.1. MA-MBR performance at low bulk VSS is governed by balancing loading rate and SRT management

After inoculation, operation of the MA-MBR started at OLR of 0.5 g COD L^{-1} d^{-1} (Phase I) and gradually increased to finally reach up to 6 g COD L^{-1} d^{-1} (Phase VII). In phase I, the reactor was underloaded and manual interventions with addition of sodium acetate spikes led to fluctuations in CODRE (77 ± 16 %). No biomass wasting was performed in this phase to prevent washout. After re-inoculation (day 36) and increase of OLR to 1 g COD L^{-1} d^{-1} (phase II), a drop of dissolved oxygen (DO) from 3.5–8 to 0.5–3.5 mg O_2 L^{-1} in the reactor indicated higher biological activity and SRT management was instated to target bulk-SRT of10 days. Under these conditions, a CODRE of 94 ± 1 % was achieved, resulting in effluent containing 36 mg COD L^{-1} (Fig. 1B) and 2.2 mg L^{-1} BOD_5 (Table 1) and a MLSS after scouring stabilizing around 0.1 g VSS L^{-1} (Fig. 1D).

When the OLR was increased to 2 g COD L^{-1} d^{-1} (Phase III), the VSS concentration in the bulk after scouring went up from 0.1 to 1.5–2 g VSS L^{-1} and ORP dropped from 150 to −300 mV. An upward trend in the effluent from 35 to 50 COD mg L^{-1} at −300 mV indicated insufficient (oxic) capacity of the system to metabolize the COD. In response, the bulk-SRT was lowered from 10 to 1 day (Phase IV) to reduce oxygen demand following from respiration while keeping an OLR of 2 g COD L^{-1} d^{-1}. In this phase, MLSS lowered from 1.5–2 to 0.4 g VSS L^{-1}, DO rose from 0 to 4–6 mg O_2 L^{-1} and ORP became positive, whilst effluent soluble COD (sCOD) went down from 50 to 35 mg L^{-1}, indicating that reducing the SRT improved the effluent quality.

To test the limits of the system, the OLR was then doubled from 2 to 4 g COD L^{-1} d^{-1} (Phase V). Oxic conditions could be maintained for the first 15 days and similar effluent quality could be produced with sCOD of 35 mg L^{-1} at DO of 1 mg O_2 L^{-1}. On day 120, the DO was depleted (0 mg O_2 L^{-1}) and ORP fell below 0 mV; further deteriorating to −400 mV at day 130. MLSS concentrations lowered throughout this decrease from 0.4 (day 100) to 0.05 g VSS L^{-1} (day 130), which indicates a lower scouring efficiency under anoxic conditions. The lack of effective biofilm management led to increased SRT in the reactor and an increased oxygen demand due to respiration. The thicker biofilm aggravated this issue by increasing the diffusion pathlength, ultimately resulting in anaerobic conditions in the liquid bulk after day 120 (ORP < 0 mV). By comparing the relative uptake of 30–50 g COD g N^{-1} to the theoretical rate of 21 at bulk-SRT of 1 day, the total SRT was assessed to be rather between 3–10 days (day 100–125), (Supplementary information G, Fig. S9). As the relative COD/N uptake after day 125 approached and even dropped below the expected value of 21 g COD g N^{-1}, heterotrophic denitrification (ORP < −200 mV) may have distorted the COD/N uptake ratio under anaerobic conditions.

The anaerobic conditions in the liquid bulk did not significantly affect effluent sCOD (35 mg L^{-1}) whilst the sCOD in the reactor liquid rose from 35 to 100 and eventually to 150 mg COD L^{-1} (day 120–140). The difference between the sCOD in the reactor and effluent shows a retention at the filtration membrane surface. After replacement of the filtration membrane due to a leak in the u-cap sealing the IPC (day 140), the effluent contained significantly more sCOD (125 mg COD L^{-1}) than before(30–50 mg L^{-1}), whilst the difference between the sCOD effluent and sCOD reactor remained similar (100–150 mg COD L^{-1}). This led to a lower sCODRE (70–80 %), which implies that the fresh membrane had a lower retention capacity for sCOD. Moreover, the sCOD effluent slowly decreased within 10 days to 50 mg L^{-1} (day 149), indicating that the sCOD retaining improved over time, and the improved retention may have led to better degradation.

In phase VI, the reversibility of the aeration membrane biofilm scouring efficiency under anaerobic bulk conditions (day 120–155) was tested. To do so, the LR was reduced to 2 g COD L^{-1} d^{-1}. As such, the ORP increased to 50–200 mV, whilst DO went from 1 to 7 mg L^{-1} (day 156–166). MLSS concentrations of 0.05 to 0.4–0.5 g VSS L^{-1} were reached after scouring, a 5–10-fold improvement over the scouring effectiveness at anaerobic conditions, showcasing a clear effect of anaerobicity in the bulk on the scouring efficiency.

In Phase VII, a short operation span was performed with a loading rate of 6 g COD L^{-1} d^{-1}. The waste flowrate was set to a target bulk-SRT of 0.5 days to prevent anaerobic conditions in the reactor, and instead of scouring, membranes were brushed before wasting events to secure effective biofilm detachment from the membranes. The first-time brushing was performed, a concentration of 1 g VSS L^{-1} was obtained (day 166), significantly higher than with scouring at any point. VSS concentrations after this initial scouring stabilized to 0.3–0.4 g VSS L^{-1}, showing that this more effective biofilm management reduced the amount of biomass in the reactor. This resulted in a higher biomass specific CODRR and more assimilation, which was also reflected by the lower COD/N uptake of 21g COD g N^{-1} (Supplementary Information G, Fig. S9) compared to other phases at oxic conditions. Throughout this phase, an ORP of 100–200 mV could be maintained, the effluent sCOD

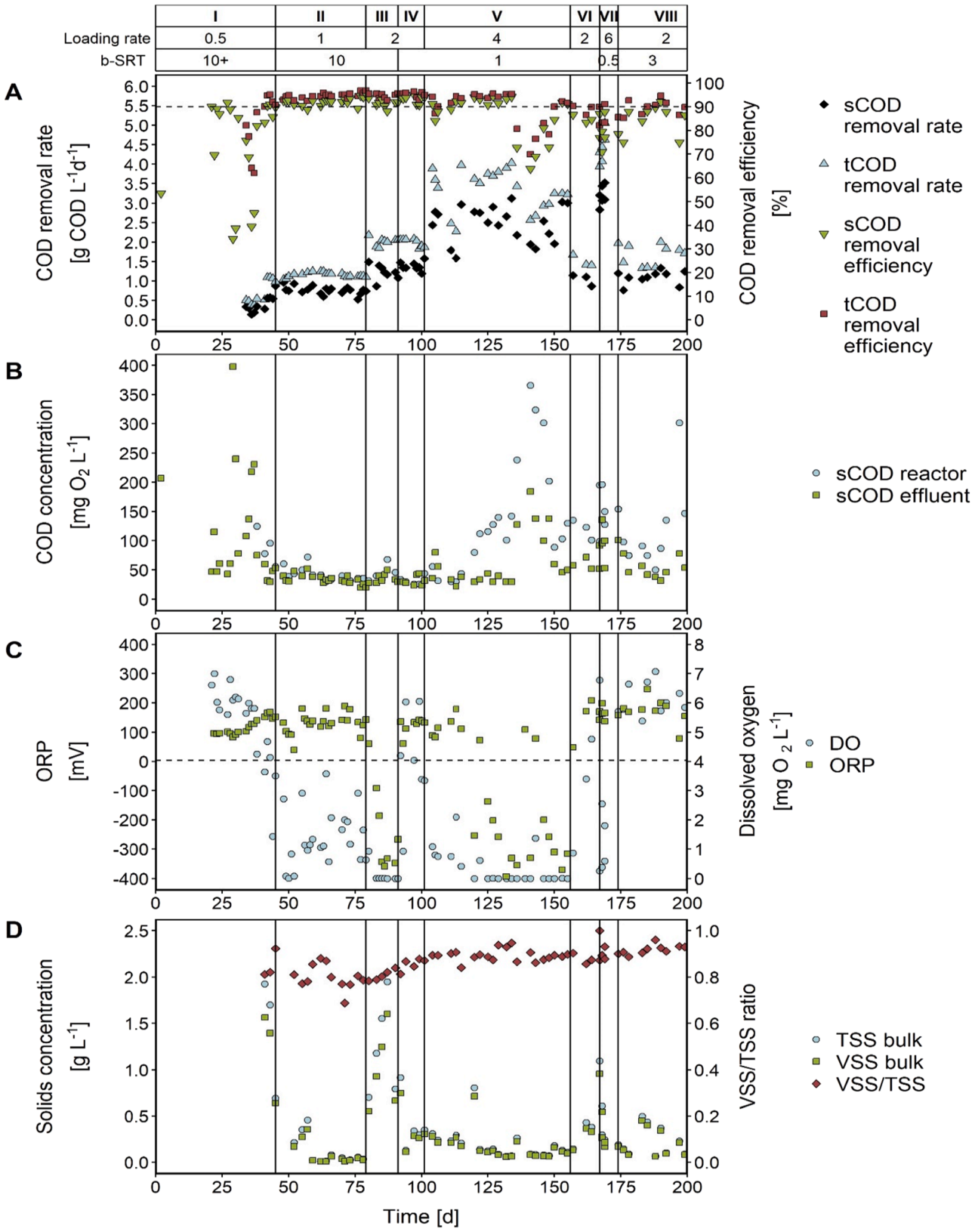

Fig. 1. Reactor performance over time. A) COD removal rates & efficiencies, B) concentration of COD in the reactor and in the effluent, C) ORP and DO in the reactor D) Total and volatile suspended solids (TSS and VSS) concentrations in the mixed liquor (bulk') after reactor scouring. Phases, organic loading rate and bulk solids residence times (bulk-SRT) are described in the header.

Table 1
Summary of main results for each condition of corrected loading rate and bulk solids retention time. The mean values and standard deviation are presented. Results from Condition IV displayed in the table were obtained prior to reactor failure (days 101 – 125). COD eff – COD in the effluent; BOD5 eff – BOD5 in the effluent; COD RE – COD removal efficiency; BOD5 RE - BOD5 removal efficiency; COD RR – COD removal rate; NRR – nitrogen removal rate.

Phase	Days	OLR g L^{-1} d^{-1}	bulk-SRT d	HRT h	COD eff mg L^{-1}	BOD_5 eff mg L^{-1}	CODRE* %	BOD_5RE* %	CODRR g L^{-1} d^{-1}	NRR g L^{-1} d^{-1}
I	1 – 40	0.62±0.00	10+	34.1±1.3	138±98	N.D.	77±16	N.D.	0.47±0.06	0.01
II	41 - 78	1.21±0.07	10	16.7±0.3	36±8	2.2±0.2	94±1	99	1.14±0.07	0.02
III	79 –90	2.10±0.09	10	9.9±0.5	34±9	3.1±0.4	95±1	99	1.95±0.24	0.04
IV	91 - 100	2.10±0.09	1.1 ± 0.6	10.1	32±7	3.2±0.3	95±1	99	1.95±0.24	0.02
V	101 - 155	3.70±0.46	1.1 ± 0.6	5.2±0.3	38±14	6.5±1.5	94±2	98	3.28±0.58	0.08± 0.04
VI	156 - 166	1.68±0.12	1.1 ± 0.6	10.4	61±8	N.D.	89±2	N.D.	1.50±0.12	0.02
VII	167 - 169	5.22±0.32	0.4 ± 0.1	3.5	90±27	14.1±2.3	84±5	95	4.41±0.37	0.12
VIII	174 - 200	1.87±0.28	3.1 ± 0.6	10.4	57±20	7.0±0.1	89±3	97	1.67±0.26	0.02

* Influent COD and BOD_5 averaged 605±66 mg L^{-1} and 300±42 mg L^{-1}, respectively.

amounted 100 ± 50 mg L^{-1} and a CODRE of only 70–90 % was reached, most likely due to biomass limitation.

A benchmark was operated with SRT of 3 days (phase VIII), in which similar sCOD levels as in phase VI were obtained. However, the increasing reactor sCOD indicated the incapacity of the sludge to biologically degrade the sCOD at the given SRT. In the separate reactor run for TMP-follow up at 4 g COD L^{-1}(Supplementary Information H, Fig. S10), the BA-MBR exhibited these biological limitations as well, and led to oxygen limitations at increased SRT, resulting in increased sCOD in the effluent to 100 mg L^{-1}. Fluctuations in sCOD were not observed in MA-MBR at b-SRT of 1 day, which performed stably throughout the operational periods at effluent sCOD <50 mg L^{-1} under anoxic bulk conditions.

2.2. MA-MBR reaches the most stringent effluent BOD_5 criteria at high loading rates

BOD_5 measurements of the effluent at different loading rates show an increase from 2.2 to 3.1 mg L^{-1} BOD_5 at OLR 1–2 g COD L^{-1} d^{-1} (Fig. 2A). At OLR 4 g COD L^{-1} d^{-1} (phase V), a concentration of maximum 6.5 mg L^{-1} BOD_5 was measured in the effluent. Notably, no difference was found between anaerobic and aerobic conditions at similar loading rates (at 2 g COD L^{-1} d^{-1}, phase III and IV, within phase 5 during oxic- and anaerobic conditions). However, at a loading rate of 6 g COD L^{-1} d^{-1}, the BOD_5 more than doubled to 14 mg L^{-1}, indicating a sludge limitation at this point. The benchmark BA-MBR was only performed at OLR 2 g L^{-1} d^{-1} using a bulk-SRT of 3 days and indicated a worse removal of BOD_5 at 7 mg L^{-1} compared to 3.1 mg L^{-1} in MA-MBR configuration.

2.3. ORP in MA-MBR regulates biological performance but has limited effect on EPS, protein, and carbohydrate content

Throughout the operation span, it was investigated whether the ORP would affect protein and carbohydrates contents of the biomass and COD in the reactor and effluent. Whereas the absolute amount of EPS harvested fluctuated strongly, effects on the biomass composition are less pronounced. An upward trend in protein over carbohydrate ratio of 2.4 at negative ORP trending towards 2.8 at positive ORP was observed, although great fluctuations of the ratio were observed in both oxic- (1–4) and anaerobic conditions (1–3) (Fig. 2B). Furthermore, slightly more EPS (0.7 g COD g VSS^{-1}) was present at negative ORP conditions than at positive ORP (0.6 g COD g VSS^{-1}).

Results for sCOD effluent and ratio at a given loading rate of 4 g COD L^{-1} d^{-1} were analyzed to exclude the effects of loading rate, bulk-SRT, and other variables (Fig. 2C&D). The sCOD in the reactor shows a negative correlation to ORP (r^2=0.45), whilst the sCOD concentration in the effluent is much less strong correlated to ORP (r^2=0.14). Whilst negative ORP in the bulk lead to accumulation of sCOD in the reactor, it did not directly affect effluent quality. Hence, the filtration membrane must have retained sCOD in anoxic conditions, likely due to its small pore size (0.04 μm vs. sCOD threshold of 0.2 μm). After replacing the filtration membrane on day 136, the sCOD in the effluent went up to over 125 mg L^{-1} (Fig. 1B) before returning to normal levels below 50 mg L^{-1} after 15 days. This indicates that the formation of a biofilm on the MBR took place, even at the low MLSS levels operated, and contributed to COD removal in effluent.

2.4. Transmembrane pressure builds up slower in MA-MBR than in BA-MBR

To assess the filtration performance in MA-MBR and compare it to BA-MBR, TMP tests were conducted over 72 h without backwashing or scouring. Both systems operated at an OLR of 4 g COD L^{-1} d^{-1}, with the MA-MBR at a bulk-SRT of 1 day and the BA-MBR initially at 1 day, later adjusted to 3 days (after day 22) to achieve comparable VSS concentrations and specific loading rates (Supplementary information H, Fig. S10)

With both TMPs starting below 0.05 bar, the MA-MBR configuration (Fig. 3A) maintained a TMP below 0.15 bar for 15 h, whereas the BA-MBR reached 0.3 bar within 2 h. In MA-MBR, TMP increased from 0.15 to 0.25 bar between 15 and 30 h, reaching 0.28 bar at 72 h. The BA-MBR TMP remained above 0.3 bar throughout the run, gradually rising to 0.35 bar, providing a first indication of a filtration advantage of approximately 25 % in MA-MBR under these highly loaded conditions.

2.5. Sludge detachment after aeration membrane scouring is ORP dependent and is followed by rapid biomass re-attachment to aeration membranes

We hypothesized that the advantage in TMP buildup could be attributed to low MLSS in MA-MBR, as we observed a drop in MLSS over time after scouring events. This could be explained by re-attachment of the suspended scoured-off biofilm fragments to the aeration membranes. To further understand this phenomenon, MLSS re-attachment tests were performed after application of shear during the different operational conditions. During operation at similar loading rate, it was observed that at low ORP, less biomass detached from the MABR at similar bulk-SRT. For respectively positive and negative ORP, VSS of 1.4 g L^{-1} vs. 0.8 g L^{-1} at SRT 10 days and 0.5 vs. 0.2 g L^{-1} at SRT 1 day was observed (Fig. 3B). The change in scoured biomass fraction might be a response of the biofilm (stratification) in the biofilm structure to lower oxygen and higher COD availability.

Then, evolution of MLSS in the next 90 min was followed to assess the floc-film behavior (attached or suspended, Fig. 3C). In all operational conditions, a steep downward gradient of MLSS after scouring was measured. After 5 min, only 50–80 % of the initial MLSS was still located in mixed liquor, whilst this reduced to 15–40 % after 25 min and >10 %

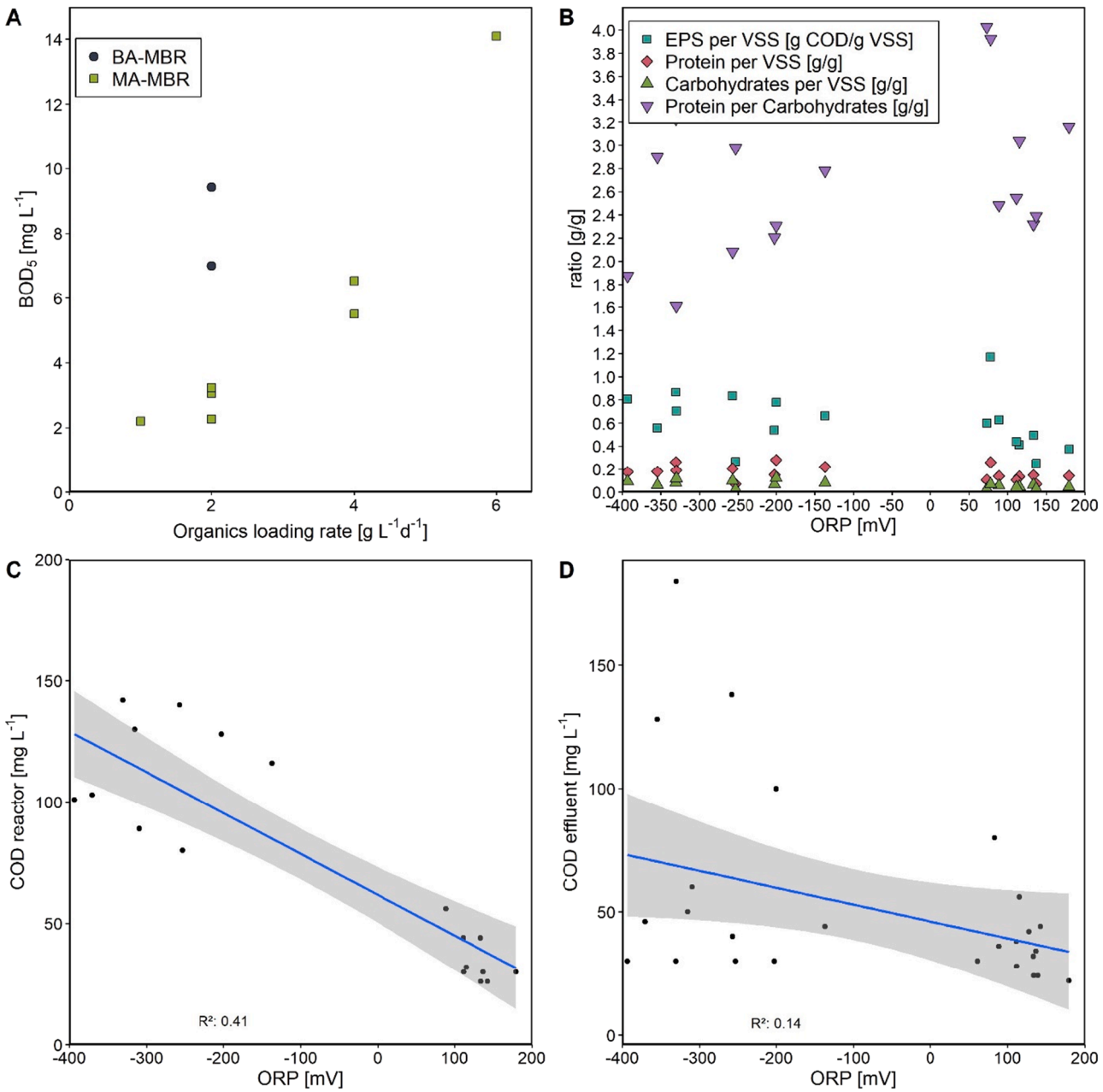

Fig. 2. Correlations between organics loading rate and effluent BOD_5 levels, between ORP and extracellular polymeric substances (EPS), and reactor and effluent COD concentrations and ORP. A) BOD_5 at the tested loading rates for the MA-MBR and the benchmark BA-MBR, B) ORP on EPS, protein and carbohydrates per VSS and protein/carbohydrates for MA-MBR at LR 4 COD g L^{-1} d^{-1}, C) relation between ORP and sCOD in MA-MBR reactor at LR of 4 g COD L^{-1} d^{-1}, D) relation between ORP and sCOD in effluent at LR of 4 g COD L^{-1} d^{-1} in MA-MBR. Trendlines for the linear regression of the datapoints are provided with the r^2 listed on the graphs. For B, C and D only data in phase V before membrane replacement are considered as to keep LR constant and exclude filtration performance from the results.

after 85 min. These data indicate that a quick re-attachment of MLSS to the aeration membrane took place in all tested scenarios, and that over 90 % of the total VSS is usually located on the aeration membranes when no scouring (e.g., biofilm management) is performed. Moreover, no significant difference in the re-attachment curve between positive or negative ORP was observed, indicating that the re-attachment phenomenon in MA-MBR on greywater does not merely depend on tested operational variables (bulk-SRT, LR).

2.6. *Microbial community in floc and film fraction significantly differs, especially at low ORP and SRT*

The microbial community was investigated throughout the operation by sampling of 1) scraped- and 2) scoured biofilm from the aeration membranes, and 3) scraped biomass from the filtration membrane, as to obtain an overview of the coverage in microbial community/similarities of the shearable fraction as part of the total fraction, which is assumed to be captioned by scraping the biofilm of the aeration membrane.

Throughout the operational run, the community quickly transitioned from the inoculum to a varying community of (aerobic) bacteria (Fig. 4A). Shannon diversity (Sh) and Pielou's evenness (Pie) within the total biofilm (AM-B) remained stable (Sh >3.5, Pie=0.6–0.7) under all operational conditions. A core community that made up 15 % of the total relative abundance in the biofilm was identified being *Acidovorax, 17J80–11(Caulobacter), Mycobacterium, Reyranella, Pseudomonas* (Supplementary Information J, Fig S11). Well-known biofilm formers

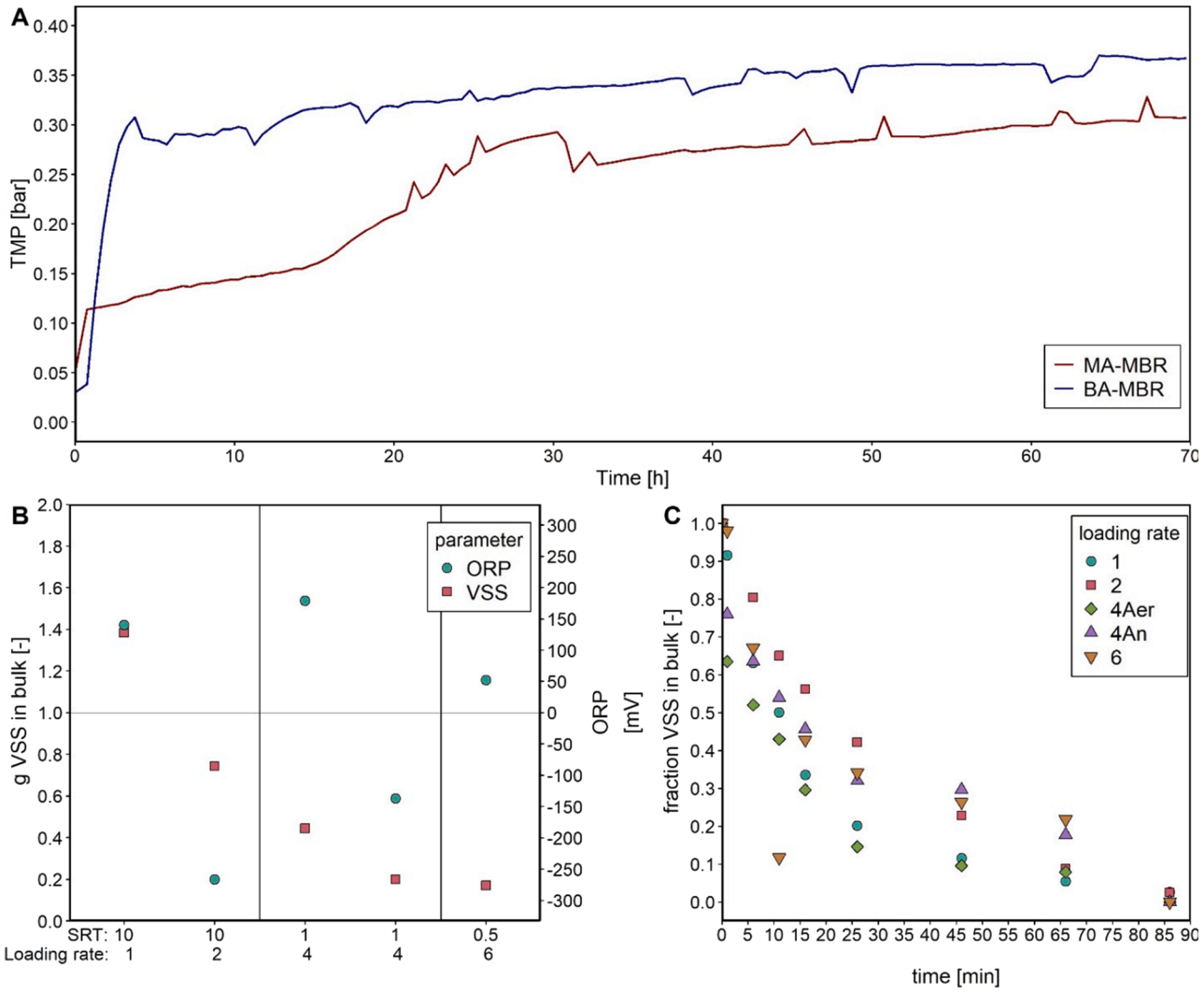

Fig. 3. Transmembrane pressure evolution and measured biomass in mixed liquor during sludge re-attachment tests. A) TMP follow up for 70 h operated at loading rate 4 g COD L^{-1} d^{-1}, at TMF of 10 L h^{-1} m^{-2}. A rolling average of the TMP per 5 min was provided to extort noise produced by the peristaltic pump, B) Resulting VSS in bulk from detachment at high and low ORP, C) Fraction of VSS in mixed liquor after application of shear at different loading rates. At loading rate 4 g L^{-1} d^{-1}, a distinction between the aerobic (Aer) and anaerobic (An) performance was made. Expressed as fraction VSS observed in bulk compared to directly after scouring.

Pseudomonas (Ghafoor, Hay and Rehm, 2011) and *Zoogloea* (Wei et al., 2023) were found. *Reyranella, Xanthobacter* (van der Kooij et al., 2020) and *Acidovorax*(Benedek et al., 2014) are described as facultative (anaerobic) biofilm formers. At low SRT, where biomass washout is more pronounced, biofilm-forming taxa appeared more abundant, suggesting that the reactor conditions select for biofilm-forming species, and that biofilm formation capacity was key for microbial proliferation in the MA-MBR biofilm. When the membranes were brushed at SRT of 0.5 days, the core community disappeared and was replaced by an uneven, low diverse community (day 168, Sh=1.5, Pie=0.34).

In contrast to the biofilm, the scoured samples exhibited greater fluctuations (Sh=2.5–3.5, Pie=0.4–0.6). These samples showed high incidental abundances of genera such as *Pseudomonas* and *Cloacibacterium*, with diversity more resembling the diversity and evenness of the benchmark (day 188, Sh=2.6, Pie=0.55). The variability between scoured and total biofilm samples suggests that only a part of the biofilm is effectively scoured off, whilst a high diversity biofilm on the aeration membrane proliferates with minimal impact of scouring and bulk conditions.

Principal component analyses (PCA) showed the largest dissimilarity of the biofilm sample at SRT 0.5 d on PC 1(43 %) =0.9 whilst all other samples were grouped closely (−0.2–0.1) (Fig. 4B). At the SRT of 0.5 days, aeration membrane brushing was performed. The results suggest that this had a heavy effect on the microbial community effectively as it detached most of the biofilm followed by washout, so that only a fast-growing community with low diversity was able to proliferate in the reactor. When only the total, scoured and filtration samples were compared without the brushed sample (Fig. 4C), a grouping of the biofilm samples around 0.0 on both PCs is observed, whilst the benchmark sample and the scoured samples vary from −0.4 to 0.5 on PC1 (33 %) and −0.5–0.3 on PC2, indicating a fluctuating and dissimilar community to the biofilm. When only the scoured and total biofilm samples were compared (Fig. 4D), the variation of the community was linked to ORP (0.45 on PC1, 41 % and 0.4 on PC2, 26 %) and SRT (0.83 on PC2). Especially the scoured samples exhibit a strong variation over PC1, which suggests the ORP affects the scoured samples more than the biofilm samples.

A correlation graph of ORP and SRT on the diversity was made to further investigate their respective effects on the total biofilm and the scoured samples. For ORP, when only samples of SRT 1 day were considered, a distinct positive trend between ORP and Shannon diversity was observed for the scoured samples from 2.7 to 3.5, whilst the total biofilm remained constant, if not decreased slightly from Sh=3.9 to 3.7 (Fig. 4E). For SRT (Fig. 4F), Shannon diversity of the scoured fraction

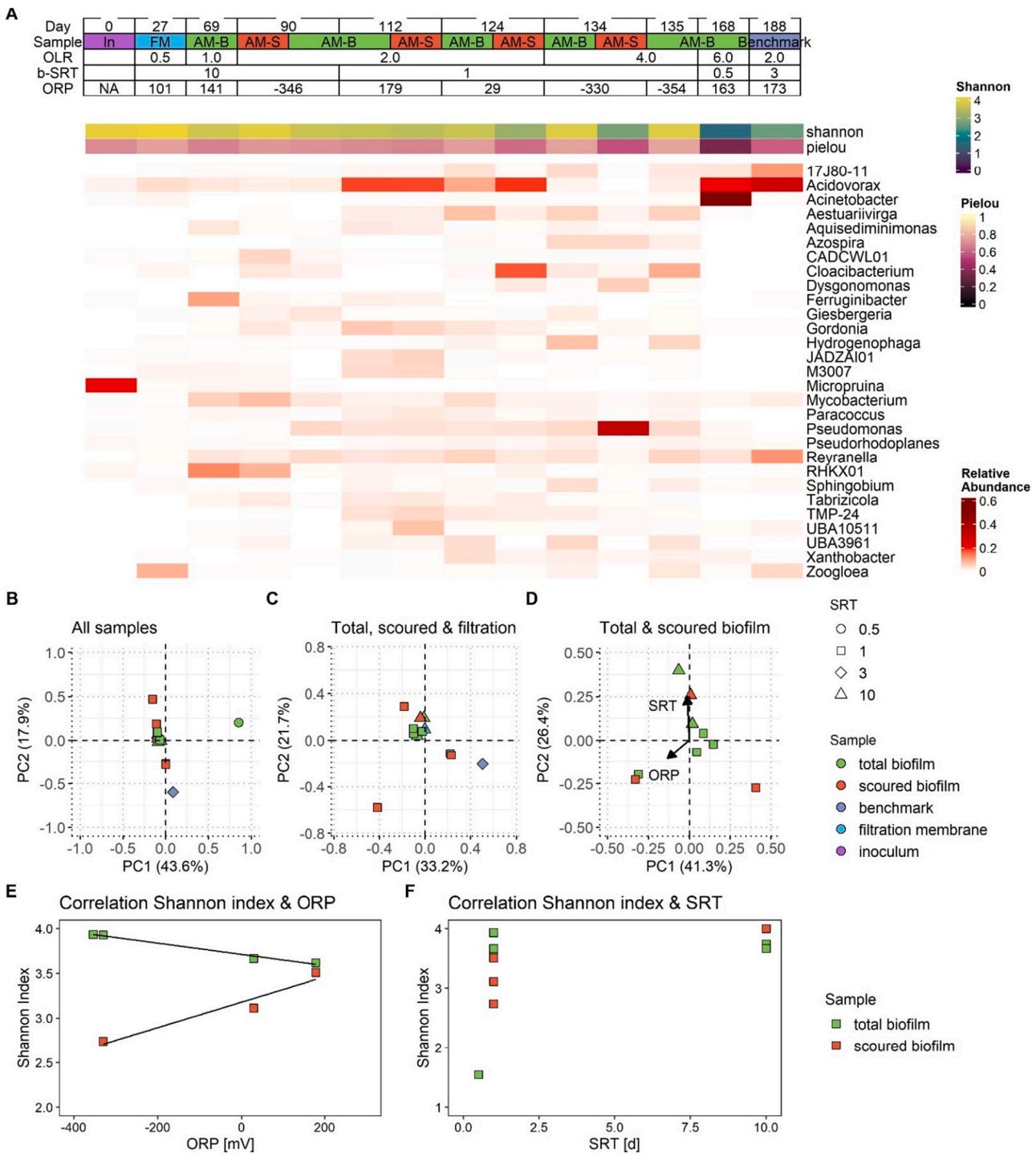

Fig. 4. Most abundant genera in and principal component analyses in the MA-MBR. A) Relative abundance of the 30 most abundant genera in the reactor. In the header, the location of sampling is given (In=inoculum, FM=filtration membrane, scraped, AM-S= aeration membrane, scoured, AM-B=Aeration membrane, biofilm). OLR and bulk-SRT at each sampling point are provided, and Shannon diversity and Pielou evenness are displayed, B) Principal component analysis (PCA) of all samples, C) PCA of samples at bulk-SRT 1,3-, and 10-days, D) PCA of scraped and scoured sludge of the aeration membrane. Arrows are displayed for correlations of principal components to ORP and SRT (scaled with factor 0.3), E) Correlation between the Shannon diversity and ORP at SRT=1d, F) Correlation between Shannon Index and SRT. Only scoured and total biofilm samples were assessed in E & F.

increases towards 4, similar to the diversity of the biofilm samples. The Shannon diversity of the biofilm samples showed no effect of SRT, except when brushing was done for SRT management (SRT= 0.5 d).

3. Discussion

3.1. MA-MBR combination reaches better removal rates than BA-MBR whilst adhering to strict effluent standards for non-potable reuse

The overall objective of this study was to assess CODRR, CODRE and effluent quality on greywater treatment with MA-MBR and to compare

them to BA-MBR. The MA-MBR could reach a maximum CODRR up to 5.5 g COD L^{-1} d^{-1} (26.8 g COD m^{-2} d^{-1}) at 70–80 % CODRE and long term CODRR at 4.0 g COD L^{-1} d^{-1} (19.5 g COD m^{-2} d^{-1}) at high CODRE of >90 %. Typical state-of-the-art MBRs for greywater treatment reach CODRR of 0.5–2 g COD L^{-1} d^{-1} (Winward et al., 2008; Judd, 2010; Paris and Schlapp, 2010), often limited by effluent requirements and by the specific oxygen transfer efficiency at high MLSS concentrations (Kim et al., 2019). The only MBR on greywater known to the authors that reached comparable CODRR of 6 g COD L^{-1} d^{-1} (Emaminejad, Avval and Bonakdarpour, 2019) required an specific aeration demand (SAD) of 5.45 m^3 m^{-2} h^{-1}, roughly 30 times the amount used in industrial applications and daily physical filtration membrane cleaning, due to intense fouling. The MA-MBR in this study could be operated at MLSS below 0.5 g L^{-1} VSS using SAD of 0.25 m^3 m^{-2} h^{-1} with the same forward/backward filtration regime as in preceding phases.

The effluent adhered to the most stringent reuse standards of 5–10 mg L^{-1} BOD_5 (Nolde, 2000; European Commission, 2022) up to loading rates of 4 g COD L^{-1} d^{-1} for domestic reuse, or for less stringent reuse quality such as irrigation of crops (Zhu and Dou, 2018). Whilst at 6 g COD L^{-1} d^{-1}, the effluent did not adhere to the most stringent reuse norms, this may be attributed to the high COD concentration in the used synthetic greywater matrix. The COD and BOD_5 concentrations of the influent in this study were ~700 mg L^{-1} COD and ~300 mg L^{-1} BOD_5, which corresponds to dark greywater, e.g. according to Larsen, Udert and Lienert, 2013, that reported respectively 620 mg L^{-1} COD and 280 mg L^{-1} BOD_5. Yet, many greywater treatment facilities report lower COD and BOD_5 concentrations, citing a strong dependence on water usage per country (Boyjoo, Pareek and Ang, 2013). Moreover, the mixture applied here originated from soaps, shampoos and laundry detergents, of which the recalcitrant nature has been reported to complicate removal (Nolde, 2000) compared to typical COD encountered in greywater, e.g. from kitchen waste. Therefore, the degree of removal achieved in this study suggests that a better effluent quality could even be reached on real water with lower concentrations of COD, potentially even reaching BOD_5-standards for most strict reuse at a LR of 6 g COD L^{-1} d^{-1}.

3.2. Low MLSS concentration due to re-attachment of flocs in ma-mbr reduces transmembrane pressure buildup from clogging

The 72-h TMP tests provide a first indication of the filtration performance differences between MA-MBR and BA-MBR under high-loading conditions. While longer-term operation is required to fully assess sustainable permeability, early stage TMP trends are known to correlate with long-term filtration membrane performance in MBRs (Fan, Zhou and Husain, 2006; Le-Clech, Chen and Fane, 2006). The observed 25 % reduction in TMP buildup suggests that MA-MBR can mitigate initial clogging rates more effectively than BA-MBR. Operation at lower MLSS and sCOD ratio reactor/effluent could play a role in the filtration performance of the clean membrane and are primary candidates to better control fouling during long-term operation.

The filtration capacity of an MBR is often influenced by submicron particles (Faust et al., 2014). The MA-MBR in this study exhibited high biological degradation efficiencies, better than the BA-MBR, evidenced by the low BOD_5 and similar sCOD in both the reactor and effluent. This suggests a minimal risk of submicron particle-induced clogging, given the filtration membrane's small pore size of 0.04 μm. The BA-MBR normally operates with high MLSS to obtain a low specific loading rate and good biodegradation efficiency, but this entails substantial extra aeration demand due to scouring, sludge respiration, and an increasing alpha factor (Judd 2010). We argue that in MA-MBR the high MLSS is not necessarily needed: Unlike BA-MBRs, which require minimum MLSS to prevent fouling, MA-MBR decouples SLR and MLSS concentration, reducing the risk of clogging.

Another explanation for enhanced filterability may lie in the size of the scoured-off biofilm fragments in MABR, which are larger than typical flocs (Corsino and Torregrossa, 2022). Strategies like densification, e.g., using hydrocyclones, have been shown to increase filterability by promoting the formation of larger flocs that are less intrusive on filtration membrane pores (Astrand, Gagnon and Peeters, 2024; Bauhs et al., 2024; Gu, 2024). The observation that 90 % of MLSS re-attaches within 60 min suggests that particle size dynamics play a role in filterability. Scouring, with the effect of biofilm fragments detaching from the aeration membrane allowing for SRT-control, followed by rapid re-attachment may prevent breakup of the biofilm fragments into fine particles (and potential release of EPS), which are known to cause membrane clogging (Van den Broeck et al., 2010). While this mechanism aligns with the improved filterability observed at lower MLSS, further analysis of particle size distributions is needed to confirm this hypothesis.

While the promising results on TMP buildup suggest a significant advantage of the MA-MBR, it is important to consider potential long-term fouling effects associated with low MLSS concentrations. Should future long-term studies find a detrimental impact of low MLSS on fouling, a feasible mitigation strategy would be to decouple the MLSS in the membrane aeration and -filtration compartments by adjusting the inner recirculation rate. This approach could increase MLSS in the filtration module, potentially preventing fouling while still maintaining reduced oxygen demand for respiration in the aeration membrane module.

3.3. SRT and ORP management are critical for optimal performance

SRT and ORP control were critical for MA-MBR performance, influencing both sCOD concentrations and effluent stability. During negative ORP, sCOD increased in the reactor, but effluent sCOD remained stable due to membrane filtration aided by a biological layer. This phase also impacted microbial community dynamics, particularly between scoured flocs and the total biofilm. Scouring primarily removed an outer layer of loosely attached flocs rather than the core biofilm, leading to distinct microbial compositions between the detached flocs and the remaining biofilm. The differences likely stem from variations in shear, oxygen presence, and H_2S accumulation under anaerobic conditions. Under negative ORP, bulk-DO depletion may have suppressed the growth of this floc community, reducing scouring efficiency and altering the microbial composition of reattached flocs.

Compared to MB-MBR, where continuous shear led to higher biofilm detachment and community homogenization (Huang et al., 2017), the intermittent shear in MA-MBR promotes phased reattachment on the membrane-aerated biofilm. This intermittent shear, combined with anoxic conditions, reinforces the separation between flocs and biofilm. Optimizing SRT through more targeted scouring and wasting based on ORP could improve oxygen supply control but may also compromise COD degradation, as seen in brushing strategies at high loading rates (6 g COD L^{-1} d^{-1}).

More investigations on how this mechanism, unique to MA-MBR, works at larger scale and how the biofilm fragments would be re-attached or dispersed in different operational regimes (e.g., with more or less shear) could shed light on the applicability of the proposed larger sludge particles and improved settleability without requirement of a densification step.

3.4. Implementation of MA-MBR in decentralized treatment trains

The results in this study indicate that MA-MBR can process up to 4 g COD L^{-1} d^{-1} (HRT= 3.5 h) for non-restricted domestic reuse. This rate is twice as high as commonly achieved in BA-MBR, whilst the effluent quality remained similar. Given the average tCOD greywater concentration of 600 mg O_2 L^{-1} used in this study, a reactor volume of only 7.4 L per inhabitant equivalent $(I.E)^{-1}$ would suffice to produce 50 L $I.E^{-1}$ d^{-1} of non-potable water that meet the highest quality requirements, which is in line with the typical non-potable reuse demand in Belgium

(VMM, 2022). Yet, a great pitfall of decentralized sanitation is the cost per treated m^3, which can exceed 4 times the treatment costs of large scale treatment (Brepols, Schäfer and Engelhardt, 2010). The MA-MBR can save 70–80 % in aeration energy. Moreover, the lower clogging rate outlines a potential for a reduction of SAD. Together, these two make up half to two-third of energy costs in BA-MBR (Fenu et al., 2010). To illustrate potential savings, consider a BA-MBR system with an aeration energy demand of 0.6–1 kWh m^{-3} (Verrecht et al., 2010). If MA-MBR achieves a 70 % reduction, this translates to a savings of 0.42–0.7 kWh m^{-3}. At an electricity price of €0.20 kWh^{-1}, this equates to a €0.08–€0.14 m^{-3} reduction in operational costs. Extrapolated to a decentralized system treating 50 I.E. at 50 L $I.E^{-1}$ d^{-1}, the savings could reach €73–€128 y $I.E.^{-1}$ in aeration costs alone, before accounting for additional benefits such as reduced maintenance and potential energy recovery. The lower SRT required for MA-MBR reduces the oxygen demand by up to 40 %,but results in more sludge production than in BA-MBR (Metcalf and Eddy et al., 2007), which needs to be managed. Digestion of the produced sludge and subsequent biogas production could be used for decentralized heating and/or electricity generation even further reducing the net energy input (Verstraete and Vlaeminck, 2011; Tervahauta et al., 2014). Whilst the here obtained data are very preliminary, a techno-economic analysis should confirm in later stages whether the footprint, maintenance and aeration advantages could offset the CAPEX associated with the addition of aeration membranes (Syron and Casey, 2008) for newly built plants or retrofitted capacity upgrades.

A major challenge of decentralized wastewater treatment is the costs associated with source separation infrastructure (Garrido-Baserba et al., 2018, 2022). As a result, some studies suggest treating non-source-separated sewage with MA-MBR for non-potable reuse may be more economically viable, especially compared to hybrid centralized-decentralized schemes (Roefs et al., 2017; Garrido-Baserba et al., 2018). However, this approach requires efficient nitrogen removal from wastewater. MABRs are known for their capacity to perform simultaneous nitrification-denitrification due to their nitrifier retention (Dong et al., 2009; Castrillo et al., 2019; Uri-Carreño et al., 2021), which would reduce need of external carbon source dosage for denitrification. For MA-MBR, this advantage has to be re-assessed as SRT-management at negative ORP was found to be more challenging. Further assessment is needed to determine the optimal loading rate for nitrogen removal and to evaluate whether the attachment-detachment mechanism on the aeration membrane remains effective.

The competitive ability of MA-MBR to remove COD from wastewater, as demonstrated in this study, expands its potential for direct water reuse applications. With its high treatment efficiency and low energy consumption, MA-MBR systems could be particularly valuable in mobile disaster response units, providing low-footprint water treatment solutions. Additionally, integrating MA-MBR with reverse osmosis (RO) systems could produce potable water with a minimal footprint.

Beyond domestic implementation, the MA-MBR advantages could be effectively applied to industrial water reuse. While domestic innovation is often limited by sunk costs and the long life expectancy of existing infrastructure (Etnier et al., 2007; Hegger, Van Vliet and Van Vliet, 2007), the industrial sector faces a stronger drive for innovation, particularly due to water security challenges during dry periods. Industrial sites are often space- and cost- constrained and produce wastewaters are rich in carbon (Hoinkis et al., 2012; Lin et al., 2012), hence could benefit from footprint advantages and energy savings of the MA-MBR technology.

4. Conclusion

- MA-MBR was operated at competitive rates of 4 g COD L^{-1} d^{-1} whilst attaining to BOD_5 and COD effluent reuse standards.
- Re-attachment of scoured flocs yielded low (>0.1 g L^{-1}) MLSS within 20 min after aeration membrane scouring, which reduced biomass exposure to the filtration membrane.
- Operation at positive ORP yielded less soluble COD filtration, potentially contributing to TMP buildup
- Short term experiments confirmed lower clogging in MA-MBR configuration compared to BA-MBR
- A distinct constant 'biofilm' and fluctuating loosely bound 'floc-film' microbial community was found on the aeration membranes, of which the floc community responded to operational conditions.

5. Materials and methods

5.1. MA-MBR experimental set-up

The reactor was composed of an aeration membrane coupled together with a filtration membrane (Fig. 5). The aeration membrane consisted of polydimethylsiloxane (PDMS) hollow fiber aeration membranes with a length of 0.92–0.96 m and a surface area of 0.78 m^2 (OxyLab 4.1, OxyMem, Ireland) contained within a 3.8 L cassette, providing a surface over volume ratio of 200 m^2 m^{-3} in line with commercial full scale plants. An extra cassette with a level detection device was added on top of the MABR. The MBR (V = 1.2 L) contained a custom-made flat sheet polyvinylidene difluoride (PVDF) ultrafiltration membrane with an Integrated Permeate Channel (IPC), pore size 0.04 µm (IPC, Blue Foot Membranes, Lommel, Belgium), tightened between two plexiglass plates and adjusted with a rubber band with an area of 0.11 m^2. The aeration membrane unit was linked to an external loop, containing probes for measuring dissolved oxygen (DO) and temperature (T) (InPro 6050, Mettler Toledo, Columbus, USA), ORPand pH, DO and T were monitored via a DO transmitter (M300 Process, Mettler Toledo, Columbus, USA) and the remaining through a pH and ORP multi-parameter controller (R3610, Consort, Belgium). The total liquid volume of the reactor was 5 L.

The influent was fed to the reactor through the external loop with a peristaltic pump (323S/D, Watson-Marlow, Marlow, UK) at a flowrate of 3.6 to 35.1 L d^{-1} depending on the loading rate. An identical pump was used for wasting. A centrifugal pump (TLCN, Lowara, Italy) was used to create a crossflow velocity to the aeration membrane of 10 cm s^{-1}, which was considered sufficient mixing to prevent any settling and to obtain reliable measurements in the external loop. A 323S/D pump was used for recirculation between aeration and filtration membrane at flowrate of 2 L min^{-1} which was assumed sufficient to prevent accumulation of biomass in the filtration module. The ultrafiltration membrane extraction pump (313 DW, Watson-Marlow, Marlow, UK) enabled effluent extraction and membrane backwashing, and TMP was measured with a pressure sensor (ATM.1ST Pressure, AE-sensors, Netherlands). An Arduino microcontroller was used to control the liquid level (TVM-FS, Atlas Scientific, New York, US), forward extraction (10 min) or backwash (1 min), and air scouring of the aeration and filtration membrane (323S/D, Watson-Marlow, Marlow, UK). The filtration membrane was designed on a maximum transmembrane flux (TMF) of 15 L m^{-2} h^{-1} and effectively reached a net flux of 1.3–13 L m^{-2} h^{-1} throughout different phases, matching the biological capacity. Membrane aeration was done from the top (countercurrent to liquid) using a pressure of ~ 1.1 bar and air flowrate of 1 L min^{-1} after it was established that a higher flowrate did not significantly impact k_La (Supplementary Information C, Fig S2). SRT management was accomplished by air scouring in the MABR (flowrate 2.35 L min^{-1}) for 5 min on a six-hour interval to release attached biomass, followed by wasting from the liquid bulk for 5 min at flowrates between 0.5 and 10 L d^{-1}, depending on the target bulk-SRT. MBR scouring was done at specific aeration demand (SAD) of 0.45 L min^{-1} or 0.25 m^3 m^{-2} h^{-1}, for the duration of the backwashing event. Further details on the control strategy are explained in Supplementary Information D. The temperature inside the reactor was maintained at 28 °C, similar to the operational temperature in a full scale decentralized

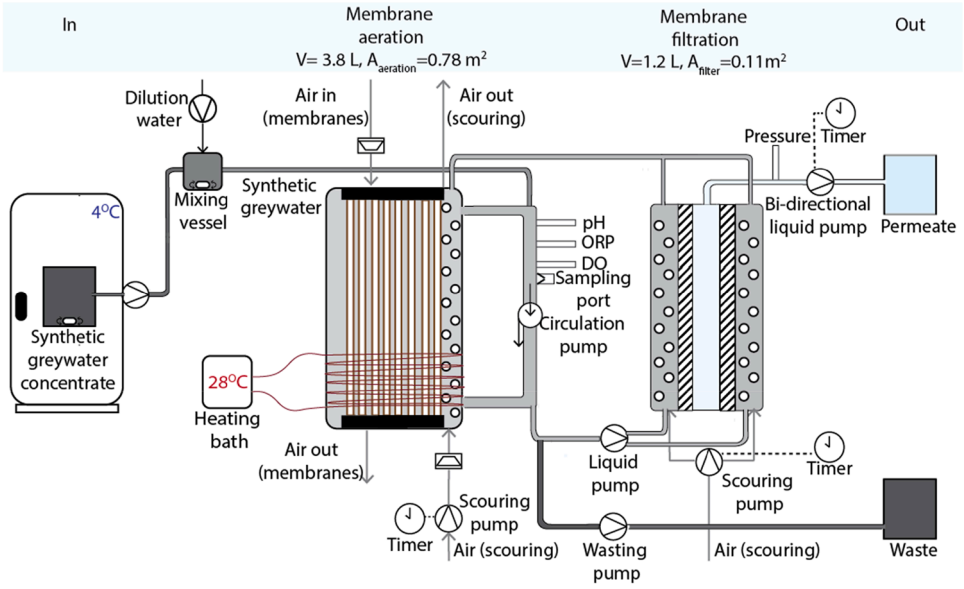

Fig. 5. process flow diagram of MA-MBR. Image provided in Supplementary Information A, Fig. S1.

treatment plant(De Nieuwe Dokken, DuCoop, Ghent, Belgium), by an immersion thermostat (A 100, Lauda, Germany), coupled to a heating water bath (DC 10/P14, Haake Technik GmbH, Germany).

5.2. MA-MBR operation

The MA-MBR was inoculated on day 1 by filling the reactor with grey- and black water digestate MBR sludge at volatile suspended solids (VSS) concentration of 4 g L^{-1} (De Nieuwe Dokken, DuCoop, Ghent, Belgium), and reinoculated on day 36 after a strong decay in MLSS due to underloading. The influent, synthetic greywater, was prepared according to NSF/ANSI 350 (2011), with a modification of the COD concentration to approximately 605 ± 66 mg L^{-1} corresponding to dark greywater which can be considered a worst-case scenario (Larsen, Udert and Lienert, 2013). Ammonium sulphate and monopotassium phosphate were added (20 mg N L^{-1} and 4 mg P L^{-1} respectively) to achieve a COD: N:P of 100:3.5:0.67, similar to dark greywater (Krishnan, Ahmad and Jeru, 2008; Hernández Leal et al., 2011). After preparation, the influent was kept refrigerated at 4 °C. The detailed composition of the synthetic greywater is described in Supplementary information B, Table S1. The reactor was operated on synthetic greywater for seven distinct conditions (I-VII) (Tab. 1) at target OLR between 0.5 and 6 g COD L^{-1} d^{-1}, corresponding to a aeration membrane specific loading rate of 2.4–29.2 g COD m^{-2} d^{-1}. Due to complications regulating the total SRT in a biofilm system, only a bulk-SRT could be set, and varied between longer than 10 and 0.5 days, over 169 days. In phase I (bulk-SRT> 10 days), no wasting was done to prevent biomass washout. During Phase VII (bulk-SRT 0.5 days), aeration membranes were brushed twice per day to ensure enough detachment. On day 140, the filtration membrane was replaced by a new identical one due to a leak in the u-caps sealing the IPC: Besides this, no filtration membrane cleaning was performed during the operational run. A benchmark with the BA-MBR was initiated on day 174 (Phase VIII), with bubble aeration. The aeration membranes were removed from the cassette and the scouring setup was used for continuous aeration with air flowrate of 0.5 L min^{-1} to achieve similar k_La to MA-MBR.

5.3.1. Sludge detachment and reattachment test

To investigate the dynamics of the MABR biofilm after scouring, detachment-reattachment tests were conducted in every operational phase. This was done by scouring the MABR biofilm for 1 min, combined to shaking the aeration membranes to simulate the turbulence of a full-scale system better. Sampling the mixed liquor was done at fixed intervals (0, 1, 6, 11, 16, 26, 36, 46, 66 and 86 min) to determine the MLSS concentration. Throughout the tests, DO in the mixed liquor was monitored and the data was logged continuously. Tests were performed on day 72,91,112,124 and 168.

5.3.2. Transmembrane pressure test

Due to filtration membrane leak issues during the long term tests, in a separate reactor-run, transmembrane pressure (TMP) evolution tests were performed for 70 h with a 0.34 m^2 filtration membrane consisting of 10 flat sheets. Both reactors were operated at a loading rate of 4 g COD $L^{-1}d^{-1}$, and performance data is provided in Supplementary Information H, Fig. S10. At the start of the tests, a chemical cleaning was performed on the filtration membrane module, by backwashing with Citric acid (0.5 %) and Hypochlorite (0.2 %) for 15 min. During these tests, scouring and backwashing were not performed to enhance resolution on TMP-evolution. A TMF of 10 L h^{-1} m^{-2} was maintained during these tests: To facilitate a continuous flowrate, an effluent recirculation loop controlled by the height sensor was installed. During the BA-MBR, run the SRT was increased from 1 to 3 days (day 22) to retain biological performance and prevent washout/too high specific sludge loading rate.

5.3. Analytical methods

COD and TN determination was performed using test kits TN 220, COD 600, and COD 1500 (Macherey-Nagel, Pennsylvania). For each condition, BOD_5 was assessed following standard procedure in the influent and effluent with addition of a nitrification inhibitor to all samples (APHA, 1998). Anions and cations were determined using ion chromatography (Metrosep A supp 5 – 150/4.0 column, ECO IC, and Metrosep C 6–150/4.0, Compact IC Flex, Metrohm, Switzerland). Details on potential measurement errors are included in Supplementary Information E, Tab. S2

On the shearable biomass, the VSS was determined every two days according to standard methods (APHA, 1998) from reactor samples obtained immediately after 5 min of MABR scouring. EPS extraction was performed in duplicate based on the modified heat method described by Van Winckel et al. (2019). Afterwards, the permeate samples were stored at −20 °C for posterior analysis of protein and carbohydrate content. Protein determination followed the Markwell method (Markwell et al., 1981), with bovine serum albumin (BSA) as standard. Carbohydrate content was determined following a method by DuBois

et al. (1956), using a glucose standard.

5.4. 16S rDNA amplicon sequencing of microbial communities

The 16sRNA was sequenced from 14 samples of the filtration membrane and aeration membrane. Three types of sludge samples were taken: Biofilm scraped from the aeration membrane (AM-B), sludge scoured from the aeration membrane (AM-S), and sludge scraped from the filtration membrane (FM). A detailed overview of the sampling can be found in Supplementary Information I, Tab. S3. For the taxonomic microbial community analysis, sludge samples were centrifuged, and the resulting pellets were stored at −20 °C prior to DNA extraction. DNA was extracted using the PowerSoil (Qiagen, Hilden, Germany) extraction kit according to the protocol provided by the manufacturer. The V4 region of the 16S rRNA gene was amplified with 341F-806R universal primers derived from (Klindworth et al., 2013) and (Caporaso et al., 2011), and sequenced on a Novaseq platform generating 250 bp paired end reads (Illumina, San Diego, California, US) by Novogene (Beijing, China). Reads were filtered using cutadapt 3.3 with a minimum length of 20, minimum overlap settings 10 and max mismatch density of 0.2. Statistics were performed in R using the Vegan package. For the heatmap, the relative abundance of the detected genera in all samples were summed, and top 30 abundant were filtered. Principal component analyses, Shannon and Pielou indices were performed on the complete dataset.

CRediT authorship contribution statement

Marijn J. Timmer: Writing – review & editing, Writing – original draft, Validation, Project administration, Methodology, Investigation, Funding acquisition, Data curation, Conceptualization. **Maria Inês Vaz:** Writing – original draft, Visualization, Investigation, Data curation. **Jolien De Paepe:** Conceptualization. **Iris Jiaqi De Corte:** Writing – review & editing, Investigation. **Marina E. Perdigão:** Resources. **Adrie J.J. Straathof:** Resources. **Tim Van Winckel:** Writing – review & editing, Writing – original draft, Supervision, Conceptualization. **Siegfried E. Vlaeminck:** Writing – review & editing, Supervision, Funding acquisition, Conceptualization.

Declaration of competing interest

The authors declare the following financial interests/personal relationships which may be considered as potential competing interests:

Marijn Timmer reports financial support was provided by Research Foundation Flanders. If there are other authors, they declare that they have no known competing financial interests or personal relationships that could have appeared to influence the work reported in this paper.

Acknowledgements

M.J.T. was supported by the Research Foundation−Flanders (Fonds Wetenschappelijk Onderzoek (FWO)) predoctoral grant 1S09022N. We deeply thank Peter Aerts & Blue Foot membranes for their kind provision of the filtration membrane module and Ine Smeekens and Noah Habers for their lab support.

Supplementary materials

Supplementary material associated with this article can be found, in the online version, at doi:10.1016/j.wroa.2025.100344.

Data availability

Data will be made available on request.

References

APHA, 1998. Standard Methods for the Examination of Water and Wastewater, 20th Edition. APHA, Washington DC.

Astrand, N., Gagnon, J. and Peeters, J. (2024) 'MABR-DAS: coupling MABR & densification for enhanced biological selection', in. Available at: https://doi.org/10.2175/193864718825159490.

Atanasova, N., et al., 2017. Optimized MBR for greywater reuse systems in hotel facilities. J. Environ. Manage 193, 503–511. https://doi.org/10.1016/j.jenvman.2017.02.041. Available at.

Bauhs, K., et al., 2024. Making waves: riding the densification wave from current understanding to advancement. Water. Res. 257, 121690. https://doi.org/10.1016/j.watres.2024.121690. Available at.

Benedek, T., et al., 2014. Analysis of biofilm bacterial communities responsible for carbon removal through a reactor cascade treating wastewater. World J. Microbiol. Biotechnol. 30, 977–987.

Boano, F., et al., 2020. A review of nature-based solutions for greywater treatment: applications, hydraulic design, and environmental benefits. Sci. Total Environ. 711, 134731. https://doi.org/10.1016/j.scitotenv.2019.134731. Available at.

Boyjoo, Y., Pareek, V.K., Ang, M., 2013. A review of greywater characteristics and treatment processes. Water Sci. Technol. 67 (7), 1403–1424. https://doi.org/10.2166/wst.2013.675. Available at.

Brepols, C., Schäfer, H., Engelhardt, N., 2010. Considerations on the design and financial feasibility of full-scale membrane bioreactors for municipal applications. Water Sci. Technol. 61 (10), 2461–2468.

Bunse, P., et al., 2023. Effects of scouring on membrane aerated biofilm reactor performance and microbial community composition. Bioresour. Technol. 369, 128441. https://doi.org/10.1016/j.biortech.2022.128441. Available at.

California Code of Regulations, 2015. Water recycling criteria. Available at https://govt.westlaw.com/calregs/Index?bhcp=1&transitionType=Default&contextData=%28sc.Default%29 (Accessed: 16 February 2024).

Caporaso, J.G., Lauber, C.L., Walters, W.A., Berg-Lyons, D., Lozupone, C.A., Turnbaugh, P.J., Fierer, N., & Knight, R. (2011). Global patterns of 16S rRNA diversity at a depth of millions of sequences per sample. *Proceedings of the National Academy of Sciences of the United States of America*, 108(SUPPL. 1), 4516–4522. https://doi.org/10.1073/PNAS.1000080107/SUPPL_FILE/PNAS.201000080SI.PDF.

Castrillo, M., et al., 2019. Mass transfer enhancement and improved nitrification in MABR through specific membrane configuration. Water. Res. 152, 1–11. https://doi.org/10.1016/j.watres.2019.01.001. Available at.

Chen, F., Bi, X., Ng, H.Y., 2016. Effects of bio-carriers on membrane fouling mitigation in moving bed membrane bioreactor. J. Memb. Sci. 499, 134–142. https://doi.org/10.1016/j.memsci.2015.10.052. Available at.

Corsino, S.F., Torregrossa, M., 2022. Achieving complete nitrification below the washout SRT with hybrid membrane aerated biofilm reactor (MABR) treating municipal wastewater. J. Environ. Chem. Eng. 10 (1), 106983. https://doi.org/10.1016/j.jece.2021.106983. Available at.

Damania, R., et al., 2017. Uncharted waters: The new Economics of Water Scarcity and Variability. World Bank Publications.

Dong, yi W., et al., 2009. Effect of DO on simultaneous removal of carbon and nitrogen by a membrane aeration/filtration combined bioreactor. J Memb Sci 344 (1–2), 219–224. https://doi.org/10.1016/j.memsci.2009.08.007. Available at.

DuBois, Michel., Gilles, K.A., Hamilton, J.K., Rebers, P.A., Smith, F., 1956. Colorimetric Method for Determination of Sugars and Related Substances. Anal. Chem. 28 (3), 350–356. https://doi.org/10.1021/ac60111a017.

Emaminejad, S.A., Avval, S.S., Bonakdarpour, B., 2019. Gaining deeper insights into the bioflocculation process occurring in a high loaded membrane bioreactor used for the treatment of synthetic greywater. Chemosphere 230, 316–326. https://doi.org/10.1016/j.chemosphere.2019.04.178. Available at.

Etnier, C., et al., 2007. Overcoming Barriers to Evaluation and Use of Decentralized Wastewater Technologies and Management. Water Environment Research Foundation.

European Commission, 2022. Commission Notice guidelines to support the application of Regulation 2020/741 on minimum requirements for water reuse 2022/C 298/01. Available at https://eur-lex.europa.eu/legal-content/EN/TXT/?uri=uriserv%3AOJ.C_.2022.298.01.0001.01.ENG&amp%3Btoc=OJ%3AC%3A2022%3A298%3ATOC (Accessed: 16 February 2024).

Fan, F., Zhou, H., Husain, H., 2006. Identification of wastewater sludge characteristics to predict critical flux for membrane bioreactor processes. Water. Res. 40 (2), 205–212.

Faust, L., et al., 2014. High loaded MBRs for organic matter recovery from sewage: effect of solids retention time on bioflocculation and on the role of extracellular polymers. Water. Res. 56, 258–266. https://doi.org/10.1016/j.watres.2014.03.006. Available at.

Fenu, A., et al., 2010. Energy audit of a full scale MBR system. Desalination. 262 (1), 121–128. https://doi.org/10.1016/j.desal.2010.05.057. Available at.

Friedler, E., Butler, D., 1996. Quantifying the inherent uncertainty in the quantity and quality of domestic wastewater. Water Sci. Technol. 33 (2), 65–78. https://doi.org/10.1016/0273-1223(96)00190-4. Available at.

Garrido-Baserba, M., et al., 2018. The economics of wastewater treatment decentralization: a techno-economic evaluation. Environ. Sci. Technol. 52 (15), 8965–8976. https://doi.org/10.1021/acs.est.8b01623. Available at.

Garrido-Baserba, M., et al., 2022. The third route: a techno-economic evaluation of extreme water and wastewater decentralization. Water. Res. 218, 118408. https://doi.org/10.1016/j.watres.2022.118408. Available at.

Ghafoor, A., Hay, I.D., Rehm, B.H., 2011. Role of exopolysaccharides in Pseudomonas aeruginosa biofilm formation and architecture. Appl. Environ. Microbiol. 77 (15), 5238–5246.

Gil, J.A., et al., 2010. Monitoring and analysis of the energy cost of an MBR. Desalination. 250 (3), 997–1001. https://doi.org/10.1016/j.desal.2009.09.089. Available at.
Gu, Y., 2024. NRR24 Abstracts. In: Nutrient recovery and removal conference. Nutrient recovery and removal. Available at https://drive.google.com/drive/folders/1Pm7-cbBD2Yc1oxG1zm-Of0n1rGieE-0_. Accessed: 23 December 2024.
Hegger, D.L., Van Vliet, J., Van Vliet, B.J., 2007. Niche management and its contribution to regime change: the case of innovation in sanitation. Technol. Anal. Strateg. Manage 19 (6), 729–746.
Hernández Leal, L., et al., 2011. Characterization and anaerobic biodegradability of grey water. Desalination. 270 (1), 111–115. https://doi.org/10.1016/j.desal.2010.11.029. Available at.
Hoinkis, J., et al., 2012. Membrane bioreactor (MBR) technology – a promising approach for industrial water reuse. Procedia Eng. 33, 234–241. https://doi.org/10.1016/j.proeng.2012.01.1199. Available at.
Huang, C., et al., 2017. Comparison of biomass from integrated fixed-film activated sludge (IFAS), moving bed biofilm reactor (MBBR) and membrane bioreactor (MBR) treating recalcitrant organics: importance of attached biomass. J. Hazard. Mater. 326, 120–129. https://doi.org/10.1016/j.jhazmat.2016.12.015. Available at.
Jiang, C.-K., et al., 2019. Effect of scrubbing by NaClO backwashing on membrane fouling in anammox MBR. Sci. Total Environ. 670, 149–157.
Judd, S., 2010. The MBR book: Principles and Applications of Membrane Bioreactors For Water and Wastewater Treatment. Elsevier.
Kim, S.Y., et al., 2019. Limitations imposed by conventional fine bubble diffusers on the design of a high-loaded membrane bioreactor (HL-MBR). Environ. Sci. Pollut. Res. 26 (33), 34285–34300. https://doi.org/10.1007/s11356-019-04369-x. Available at.
Krishnan, V., Ahmad, D., Jeru, J.B., 2008. Influence of COD: N: P ratio on dark greywater treatment using a sequencing batch reactor. J. Chem. Technol. Biotechnol. 83 (5), 756–762.
Larsen, T., Udert, K., Lienert, J., 2013. Source Separation and Decentralization For Wastewater Management. Iwa Publishing.
Le-Clech, P., Chen, V., Fane, T.A., 2006. Fouling in membrane bioreactors used in wastewater treatment. J. Memb. Sci. 284 (1–2), 17–53.
Lee, E.-J., et al., 2013. Influence of sodium hypochlorite used for chemical enhanced backwashing on biophysical treatment in MBR. Desalination. 316, 104–109.
Lin, H., et al., 2012. Membrane bioreactors for industrial wastewater treatment: a critical review. Crit. Rev. Environ. Sci. Technol. 42 (7), 677–740. https://doi.org/10.1080/10643389.2010.526494. Available at.
Mainardis, M., et al., 2022. Wastewater fertigation in agriculture: issues and opportunities for improved water management and circular economy. Environ. Pollut. 296, 118755. https://doi.org/10.1016/j.envpol.2021.118755. Available at.
Markwell, M.A., Haas, S.M., Tolbert, N.E., Bieber, L.L., 1981. Protein determination in membrane and lipoprotein samples: Manual and automated procedures. Methods Enzymol. 72, 296–303. https://doi.org/10.1016/s0076-6879(81)72018-4.
Metcalf, Eddy, I., et al., 2007. Water Reuse. McGraw-Hill Professional Publishing United States of America.
Nolde, E., 2000. Greywater reuse systems for toilet flushing in multi-storey buildings – over ten years experience in Berlin. Urban Water 1 (4), 275–284. https://doi.org/10.1016/S1462-0758(00)00023-6. Available at.
Noutsopoulos, C., et al., 2018. Greywater characterization and loadings – Physicochemical treatment to promote onsite reuse. J. Environ. Manage 216, 337–346. https://doi.org/10.1016/j.jenvman.2017.05.094. Available at.
Paris, S., Schlapp, C., 2010. Greywater recycling in Vietnam — Application of the HUBER MBR process. Desalination. 250 (3), 1027–1030. https://doi.org/10.1016/j.desal.2009.09.099. Available at.
Pearce, G., 2008. Introduction to membranes: an introduction to membrane bioreactors. Filtrat. Separ. 45 (1), 32–35. https://doi.org/10.1016/S0015-1882(08)70028-4. Available at.
Roefs, I., et al., 2017. Centralised, decentralised or hybrid sanitation systems? Economic evaluation under urban development uncertainty and phased expansion. Water. Res. 109, 274–286. https://doi.org/10.1016/j.watres.2016.11.051. Available at.
Sedlak, D., 2014. Water 4.0. Yale University Press. Available at http://www.jstor.org/stable/j.ctt5vksm5 (Accessed: 10 December 2024).
Stricker, A.-E., et al., 2011. Pilot scale testing of A new configuration of the membrane aerated biofilm reactor (MABR) to treat high-strength industrial sewage. Water Environ. Res. 83 (1), 3–14. https://doi.org/10.2175/106143009X12487095236991. Available at.
Syron, E., Casey, E., 2008. Model-based comparative performance analysis of membrane aerated biofilm reactor configurations. Biotechnol. Bioeng. 99 (6), 1361–1373. https://doi.org/10.1002/bit.21700. Available at.
Syron, E., Heffernan, B., 2017. OxyMem, the flexiable MABR. Proc. Water Environ. Feder. 2017 (3), 650–656.
Tervahauta, T., et al., 2014. Improved energy recovery by anaerobic grey water sludge treatment with black water. Water. (Basel) 6 (8), 2436–2448.
Uri-Carreño, N., et al., 2021. Long-term operation assessment of a full-scale membrane-aerated biofilm reactor under Nordic conditions. Sci. Total Environ. 779, 146366. https://doi.org/10.1016/j.scitotenv.2021.146366. Available at.
Van den Broeck, R., et al., 2010. The impact of deflocculation–reflocculation on fouling in membrane bioreactors. Sep. Purif. Technol. 71 (3), 279–284. https://doi.org/10.1016/j.seppur.2009.12.006. Available at.
van der Kooij, D., Veenendaal, H.R., Italiaander, R., 2020. Corroding copper and steel exposed to intermittently flowing tap water promote biofilm formation and growth of Legionella pneumophila. Water Res. 183, 115951.
Van Winckel, T., Liu, X., Vlaeminck, S.E., Takács, I., Al-Omari, A., Sturm, B., Kjellerup, B. V., Murthy, S.N., De Clippeleir, H., 2019. Overcoming floc formation limitations in high-rate activated sludge systems. Chemosphere 215, 342–352. https://doi.org/10.1016/j.chemosphere.2018.09.169.
Verrecht, B., et al., 2010. The cost of a large-scale hollow fibre MBR. Water. Res. 44 (18), 5274–5283. https://doi.org/10.1016/j.watres.2010.06.054. Available at.
Verstraete, W., Vlaeminck, S.E., 2011. ZeroWasteWater: short-cycling of wastewater resources for sustainable cities of the future. Int. J. Sustain. Develop World Ecol. 18 (3), 253–264.
VMM, 2022. Waterverbruik huishoudens — Vlaamse Milieumaatschappij. Available at https://www.vmm.be/sectoren/huishoudens/waterverbruik-huishoudens (Accessed: 10 September 2024).
Wei, J., et al., 2023. Insight into biofilm formation of wastewater treatment processes: nitrogen removal performance and biological mechanisms. Sci. Total Environ. 903, 166550.
Winward, G.P., et al., 2008. A study of the microbial quality of grey water and an evaluation of treatment technologies for reuse. Ecol Eng 32 (2), 187–197. https://doi.org/10.1016/j.ecoleng.2007.11.001. Available at.
Yang, S., et al., 2009. Comparison between a moving bed membrane bioreactor and a conventional membrane bioreactor on membrane fouling. Bioresour. Technol. 100 (24), 6655–6657.
Zhu, Z., Dou, J., 2018. Current status of reclaimed water in China: an overview. J. Water Reuse Desalin. 8 (3), 293–307. https://doi.org/10.2166/wrd.2018.070. Available at.